Journal of Ceramic Processing Research. Vol. 4, No. 3, pp. 105~108 (2003)

J O U R N A L O F
Ceramic Processing Research

Detection of defects in CZ Si wafers by light scattering tomography

Tomoya Ogawa[a] and Nobuhito Nango[b]
[a]*Laboratory for Physics and Technology of Crystals, 2-14-1-202, Shin-sayama, Saitama 350-1331, Japan*
[b]*Ratoc System Engineering, 540 Waseda-tsurumakicho, Shinjuku-ku, Tokyo 162-0041, Japan*

Improving the quality of Czochralski method grown (CZ) Si wafers is one of the ever-lasting and very important problems to be solved. Since the keys for this improvement are effective characterization of the crystals, many ways have been developed and reported already. While light scattering tomography or laser scanning tomography (LST) to be discussed here is only one of these methods, it is very useful to detect micro-precipitates and tiny defects in the crystals such as oxygen precipitates or micro-bulk defects (MBD), aggregated vacancies (COP) and entangled dislocations in silicon crystals and misfit dislocations located between substrates and epitaxial layers.

Key words: CZ Si wafer, Detection of defects, Light scattering tomography, Optical dark field imaging, Photo-luminescence tomography.

Introduction

Since optical detection of defects is non-contacting and non-destructive ways, light scattering or laser scanning tomography (LST) [1-4], Brewster angle illumination LST [5, 6], inside total reflection at a mirror polished wafer surface [7], optical particle profiler (OPP) [8], and optical shallow defect analyzer (OSDA) [9] have been developed for defect recognition in Si wafers grown by Czochralski method or CZ Si wafers. These techniques and methods have their own merits but no one of them is preeminent and they will be complementally and cooperatively used with each other or with other methods such as transmission electron microscopy (TEM) and scanning electron microscopy (SEM).

Here, the ultimate usage and detectable limit of infrared (IR-) LST will be discussed to detect defects in CZ Si wafers in terms of

(a) Photo-luminescence tomography (PLT) due to IR-laser scanning is very effective to detect a few and tiny defects which act as killer centers of PL,

(b) The detection limit of IR-LST is equal to that of elastic scattering centers that are confirmed as particles of 10 nm in diameter,

(c) Brewster angle illumination LST is very useful to detect misfit dislocations located between an epitaxially grown layer on a substrate crystal.

Photo-luminescence tomography (PLT)

In a p-type CZ silicon wafer, the 1.06 μm radiation from a Nd-YAG laser induces photoluminescence (PL) due to recombination between the optically-induced electrons and holes and its spectrum is shown in Fig. 1. Since most defects in CZ Si wafers will act as killer centers for PL, intensity mapping of PL shows defects such as Fig. 2b within a diffusible region of the carriers that is experimentally estimated to 120 μm at room temperature. The surveillance volume of this PL mapping is determined by the carrier diffusion distance around the laser beam, that is 120 μm × 2=240 μm or more, and by the scanning distance of the beam. The PL mapping or PL tomography is, therefore, very effective to detect a few defects because the volume of PLT is much larger than that of LST when a highly sensitive PL sensor is used.

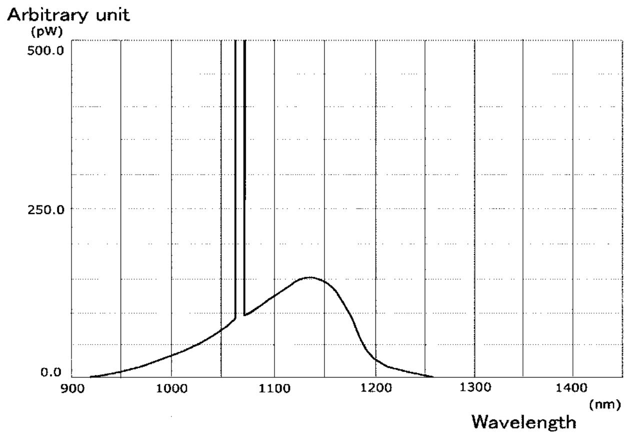

Fig. 1. PL spectrum from CZ Si under illumination of a Nd:YAG laser: 1.06 μm.

By elimination of the elastically scattered light, large dark spots were more clearly observed in a CZ Si wafer as shown in Fig. 2b. After detection of these spots, every spot is studied by layer-by-layer tomography

*Corresponding author:
Tel : +81-090-2475-2169
Fax: +81-42-969-3028
E-mail: tomoya.ogawa@gakushuin.ac.jp, nango@ratoc.co.jp

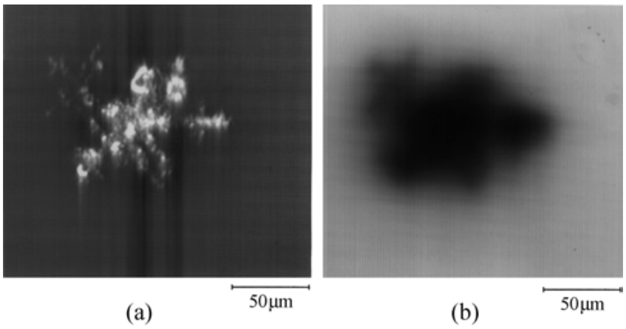

Fig. 2. Entangled dislocation observed by elastic scattering (a) and PL (b).

at 10 μm intervals by the elastic scattering using a laser beam of 4 μm in diameter [10]. By compilation of the several tomographs it is confirmed that the PL dark spot is caused by a swirled or entangled dislocation lines as shown in Fig. 2a.

Slip planes and stacking faults, which were located within oxidation-induced stacking fault (OSF) regions as estimated from their growth conditions, were observed by PLT before heating to prepare denuded zones and oxygen particles. These imaging techniques are extremely important to crystal physics of CZ Si wafers.

Detectable size limit of IR-LST

To quantitatively determine the minimum size of precipitates, the laser beam for illumination was adjusted to 4 μm in a Si wafer and an interference filter was used for correct intensity measurements to pass only the elastic component, eliminating the PL.

The data acquisition window was a narrow and long rectangle, its width along the y-axis was usually a few pixels while its length along the x-axis was 480 pixels [4], where the laser bean was parallel to the x-axis. Here, the data within the rectangular slit were acquired and stored into the memory of the computer. This process was successively continued from the initial to final positions which were correspondent with the 1st and 480th pixel position on the y-axis, respectively [3]. To improve the ratio of signal to noise, integration of the signal or multiplicity of the data acquisition was chosen as 40 to 80 times per pixel, that is, a 12 bits or 16 bits data acquisition system was used.

To correct the intensity decrement due to the beam attenuation within the specimen, all the scattered light intensities at a given x-value were summed up along the y-axis from the initial to the final position. To determine the normal decrement of the illumination in the crystal as a function of x, every value of intensity is summed up along the y-axis as a function of x, which is applied by the least squares fitting method to the equation:

$$\boldsymbol{I} = \boldsymbol{I}_0 \exp(-\alpha \boldsymbol{x}). \quad (1)$$

under assumption that scatterers are randomly and uniformly distributing within the wafer. The attenuation coefficient α was, therefore, determined by this way. The correct LST picture and the most reliable scattered intensity mapping were obtained by the correction using α.

Table 1. Diameter: a of oxygen precipitates against duration at 1000ºC

Sample	Duration	Diameter	a^2
T_{10}	10 minutes	9.8 nm	96 nm^2
T_{120}	120	28.8	829
T_{240}	240	45.4	2060
T_{360}	360	55.2	3050

To make a standard sample for quantitative determination of the detectable minimum size, a (001) CZ Si wafer heated properly was cleaved into a few fragments and diameters of twenty oxygen precipitates within one of these fragments were directly measured by TEM and their mean sizes were obtained as a_R = 29.8 nm.

Assuming that the precipitates within the other fragments were completely similar to those within the directly measured fragment, the scattered light intensity from the other one of the fragments is measured and indicated by $\boldsymbol{I_{ref}}$.

Scattered intensities from the following four wafers: T_{10}, T_{120}, T_{240} and T_{360} which were respectively heated at 1000ºC from 10 to 360 minutes after the initial heat treatment (700ºC and 4h), were measured under the eliminated PL situation. Diameters of the precipitates grown by the treatments were determined by the ratio: $\boldsymbol{I} / \boldsymbol{I_{ref}}$ under the assumption that the scattered intensity is proportional to the sixth power of its diameter or to a^6. The observed diameter a is listed in Table 1 and a^2 is plotted in Fig. 3 as a function of the duration because increment of a^2 will be proportional to the duration time at 1000ºC if the material transportation is caused by thermal diffusion process.

From Fig. 3 the two evidences are confirmed: (1) the diameter was correctly measured as small as 10 nm and (2) the oxygen precipitates were grown by the thermal

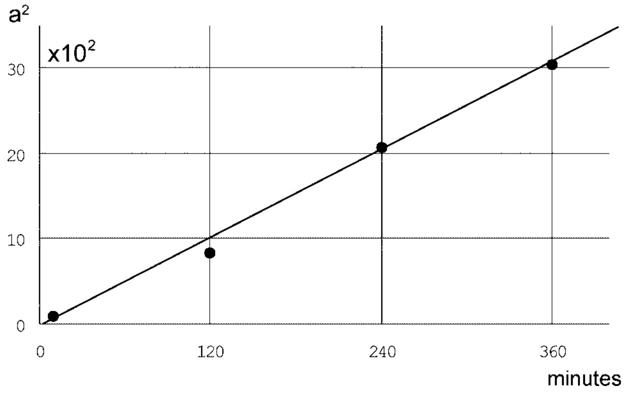

Fig. 3. The square of diameter plotted against duration time.

diffusion process due to the interstitial oxygen atoms within the CZ Si wafers.

Brewster angle illumination LST to detect misfit dislocations

Light scattering factor of an edge dislocation line

Since strains around an edge dislocation line induces special modulation of the refractive index around the line, the dislocation line is a sort of phase object. The light scattering factor of an edge dislocation line is calculated as a phase object and the square of its value is given per unit length by

$$F^2 = [\mathbf{b}^2\lambda^2\kappa^2/(8\pi^2)][(1-2\upsilon)/(1-\upsilon)]^2[g_y{}^2/(g_x{}^2+g_y{}^2)] \quad (2)$$

where the line is located along the Z axis, its Burgers' vector **b** is parallel to the X axis, and the Y axis is perpendicular to both the axes (11). Here, λ, υ and κ are respectively the wavelength of the illuminating laser, the Poison's ratio and a sort of photo-elastic constant of the crystal. When g_x is zero or the beam is perpendicular to the plane determined by the line and the vector: **b**, the factor: F^2 becomes to the maximum value and the scattered light intensity usually becomes to good enough magnitude of detection or the line is observed [11].

Brewster angle illumination

Since the refractive index of silicon crystals is about 3.5, the amplitude reflected at normal incidence of a mirror-polished Si surface is a little larger than 50%, that is too high to receive light signals scattered by defects within the crystal under normal illumination. Brewster angle illumination is, therefore, developed because the p-component reflectance of an incident beam is theoretically zero at this angle, which is very hopeful to illuminate the inside of Si wafers. Here, the Brewster angle is given by $\tan^{-1}$ n ≒ 74° (n: the refractive index).

Since the backside of a Si wafer is usually so rough that it introduces very harmful light scattering there, visible or very near IR light is chosen for illumination to completely attenuate the incident intensity before it reaches the backside. Here, a semiconductor laser diode of 800 nm wavelength is used to detect the very weak signals caused by defects under this improved S/N ratio situation.

Observation of misfit dislocations

The quality of epitaxial layer stacks such as SiGe heterojunction bipolar transistors (HBT's) was checked non-destructively by Brewster angle LST. Dislocations were detected and demonstrated in Figs. 4(a) and (b), where the direction of the incident beam is marked by a double arrow.

Here, Figure 4(d) is a combined image from Figs. 4(a) and (b) which gives us the whole misfit dislocation array perpendicular to each others which are respectively shown by the double arrows. Therefore, Fig. 4(d) is the complete arrangement of misfit dislocations in the hetero-epitaxial SiGe layer [12].

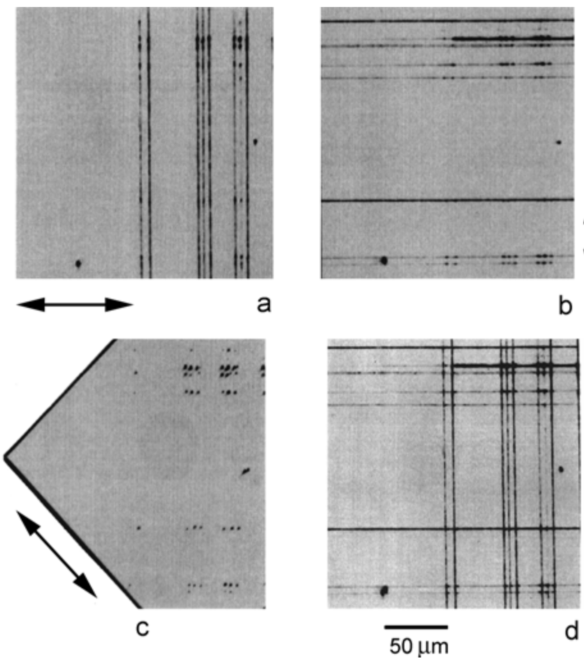

Fig. 4. The misfit dislocations observed in a SiGe heterojunction bipolar transistor by Brewster angle LST.

When the incident beam direction makes 45 degrees against the misfit dislocation line systems, only crossing points act as the scattering centers as shown in Fig. 4(c) that indicates the correctness of the analytical result: Eq. (2).

Conclusions

The origin of light scattering is a spatial deviation of magnitude of dipole radiation induced by incident light, that is, density deviation and/or fluctuation of polarizable electrons caused by irregularity due to dopants, substitutional and interstitial atoms, including irregularity due to dislocation lines will be observed by dark field imaging such as ultra-microscopy and Brewster angle illumination.

References

1. T. Ogawa, Proc. DRIP-1, Materials Sci. Monographs 31 (1985) 1-24.
2. K. Moriya and T. Ogawa, Jpn. J. Appl. Phys. 22 (1983) L207-L209.
3. T. Ogawa and N. Nango, Rev. Instrum. 57 (1986) 1135-1139
4. T. Ogawa, G. Kissinger and N. Nango, Electrochem. Soc. Proc. 97-12 (1997) 132-146.
5. T. Ogawa et al, Materials Sci. and Eng. B20 (1993) 172-174.
6. Lu Taijin, K. Toyoda, N. Nango and T. Ogawa, J. Crystal Growth 114 (1991) 64-70.
7. N. Nango, H. Furuya, J. Furukawa and T. Ogawa, J. Appl.

Phys. 78 (1995) 2892-2893.
8. K. Nakai and H. Harada, Oyo Buturi 65 (1996) 1160-1161 (in Japanese).
9. K. Takeda, H. Ishida and A. Hirayama, Mat. Res. Symp. Proc. 442 (1997) 37-42.
10. N. Nango, S. Iida and T. Ogawa, J. Appl. Phys. 86 (1999) 6000-6004.
11. K. Moriya and T. Ogawa. Phil. Mag. A 41 (1980) 191-200.
12. G. Kissinger et al., J. Crystal Growth 158 (1996) 191.